DIPOLE RADIATION PATTERN IN THE PRESENCE OF BEAM FOCUSING STRUCTURES

K. Rambabu* and **J. Bornemann**

Department of Electrical and Computer Engineering
University of Victoria, Victoria, B.C., Canada V8W 3P6

Abstract: The analysis for a dipole radiation pattern in the presence of a beam focusing structure is presented. The far field radiation pattern of the dipole in the azimuth plane is compared with simulated results using the commercial software package FEKO of EMSS. The results are found in good agreement with the FEKO's MOM based solution.

I. INTRODUCTION

Any practical antenna must operate in an environment which may consist of a variety of structures, such as the ground, aircrafts, ships, buildings, satellites, etc. The presence of such structures may cause interference in various ways, e.g., blockage of the antenna beam, etc. These may change in the antenna characteristics and especially the far field pattern. Therefore, the antenna characteristics need to be reevaluated taking into account the influences of the surroundings.

Using high frequency techniques, models have been developed to analyse configurations such as a monopole on a ground plane [1], a microstrip patch antenna on a finite PEC ground plane [2,3], a monopole on a finite cylinder [4] and a rocket shaped body [5].

In this paper, the analysis of the far field radiation pattern of a dipole in the presence of a beam focusing structure is presented. In order to increase the gain of the dipole and narrow the radiation pattern in the azimuth plane, a reflector consisting of three plates is introduced (Fig. 1). By moving the side plates back and forth, different gains can be achieved. These antennas find applications in point-to-point communication systems and in cellular base stations.

The analysis is based on a ray technique and can be extended to terrain scattering and propagation modeling, which is very important in the design and evaluation of ground-to-ground and ground-to-air communication links, as well as to low altitude radar.

Section II presents the analysis of the problem. Section III presents the results for typical structure.

II. THEORY

Fig. 1 shows the beam focusing structure including different ray paths. Here we present the two-dimensional analysis. The asymptotic evaluation of Maliuznet's exact solution using the method of steepest descent decomposes the integral solution into individual scattering mechanisms. The extracted terms include the incident field, the singly reflected field, the multiply reflected fields and the diffracted fields. Multiply reflected fields of any order with the wedge can be reduced to products of planar reflection coefficients [6]. The total field at any point is a super position of the incident, reflected, diffracted fields from edges and the surface waves. No surface waves are excited at normal incidence. Here, in order to simplify the analysis, we neglect the diffracted fields which are weaker compared to the incident and reflected fields.

0-7803-7330-8/02 $17.00 © 2002 IEEE

a) Incident Fields

For finite length wires, the total radiation will be obtained as a superposition of radiation from very small linear current elements of length Δl and constant electric current $\mathbf{I}_e = \mathbf{a}_z I_e$. This is usually referred to as the infinitesimal dipole. The radiation of the other sources can be obtained by knowing the radiation from an infinitesimal dipole. The radiation field for an infinitesimal dipole is well known and can be written as $E_{in} = I_e|\sin\theta|[\exp(-jkr)]/r$, where θ is elevation angle, r the distance between the dipole and the observation point, and k the propagation constant. In the azimuth plane, $\theta = 90^o$, so that $\sin\theta = 1$ and, assuming a unit current, the radiated field becomes $E_{in} = [\exp(-jkr)]/r$. This incident field is available in the far field, if there are no geometrical obstructions.

b) Singly Reflected Fields

The singly reflected field will reach the observation point from different places on the structure (c.f. Fig.1).

1) *From the back plate:* A ray generated from the source at origin will reach the point say (-d,y) on the back plate and reflect back to the far field point of observation. Let the far field point be $P(\rho,\phi)$. Then coordinate y can be written as

$$y = \frac{d\rho\sin\phi}{\rho\cos\phi + 2d} \geq \frac{wd}{2(h+d)} \tag{1}$$

and the far electric field is

$$E_b = \frac{\exp(-jk[\sqrt{y^2+d^2} + \sqrt{(\rho\cos\phi + d)^2 + (\rho\sin\phi - y)^2}])}{\sqrt{(y^2+d^2)[(\rho\cos\phi + d)^2 + (\rho\sin\phi - y)^2]}} \tag{2}$$

where the difference between the exponential expression and the denominator is due to the multiplication of the individual paths.

2) *From the side plate*: If (h-d)>0, fields reflected from the side plate will exist. If the ray from the source strikes the side plate at a point (x,-w/2), and after reflection it reaches $P(\rho,\phi)$, then the coordinate x can be calculated using Snell's boundary condition

$$x = \frac{w\rho\cos\phi}{2(\rho\sin\phi + w)} < (h-d) \tag{3}$$

The reflected field at the point of observation is

$$E_s^1 = \frac{\exp\left(-jk\left[\sqrt{x^2+\left(\frac{w}{2}\right)^2} + \sqrt{(\rho\cos\phi - x)^2 + \left(\rho\sin\phi + \frac{w}{2}\right)^2}\right]\right)}{\sqrt{\left(x^2+\left(\frac{w}{2}\right)^2\right)\left[(\rho\cos\phi - x)^2 + \left(\rho\sin\phi + \frac{w}{2}\right)^2\right]}} \tag{4}$$

c) Multiple Reflected Fields

Multiple reflected fields will reflect at different points in the structure and then reach the observation point. The second order reflected fields can be found as follows.

1) *Reflection from side plate to back plate and then to far field*: The ray starts from the source, strikes the side plate first and is then reflected to the back plate. After reflection at back plate, it will reach the far field. Let the ray strike the side plate at a point (x,-w/2). Then, applying Snell's boundary condition, we find

$$x = -\frac{w(\rho\cos\phi + 2d)}{2(\rho\sin\phi + w)} \qquad -d < x < -\frac{h+d}{3} \tag{5}$$

After the first reflection, the ray strikes the back plate at a point (-d,y), and the corresponding value of the y coordinate can be calculated from Snell's law.

$$y = -\left(\frac{w(x+d)}{2x} + \frac{w}{2}\right) \tag{6}$$

The electric field after two reflections - one at the side plate and one at the back plate - will reach the far field which can then be written as

$$E_{sb}^{II} = \frac{\exp\left(-jk\left[\sqrt{x^2 + \left(\frac{w}{2}\right)^2} + \sqrt{(x+d)^2 + \left(y + \frac{w}{2}\right)^2} + \sqrt{(\rho\cos\phi + d)^2 + (\rho\sin\phi - y)^2}\right]\right)}{\sqrt{\left[x^2 + \left(\frac{w}{2}\right)^2\right]\left[(x+d)^2 + \left(y + \frac{w}{2}\right)^2\right]\left[(\rho\cos\phi + d)^2 + (\rho\sin\phi - y)^2\right]}} \tag{7}$$

2) *Reflection from back plate to side plate and then to far field:* The ray starts from the source, strikes the back plate at point (-d,y), strikes the side plate at (x,-w/2) and then reaches the far field at (ρcosϕ, ρsinϕ). The x and y coordinates are

$$x = -\frac{2d\left(\rho\sin\phi + \frac{w}{2}\right) + \frac{w}{2}\rho\sin\phi}{\rho\sin\phi + w} \qquad y = \frac{\rho\sin\phi + \frac{w}{2}}{\rho\cos\phi - x}(x+d) - \frac{w}{2} \tag{8}$$

and the condition for the existence of this second order reflected field is

$$-\frac{w}{2} < y < -\frac{wd}{2(h+d)} \tag{9}$$

The electric far field can then be written as

$$E_{bs}^{II} = \frac{\exp\left(-jk\left[\sqrt{y^2 + d^2} + \sqrt{(x+d)^2 + \left(y + \frac{w}{2}\right)^2} + \sqrt{(\rho\cos\phi - x)^2 + \left(\rho\sin\phi - \frac{w}{2}\right)^2}\right]\right)}{\sqrt{\left[y^2 + d^2\right]\left[(x+d)^2 + \left(y + \frac{w}{2}\right)^2\right]\left[(\rho\cos\phi - x)^2 + \left(\rho\sin\phi - \frac{w}{2}\right)^2\right]}} \tag{10}$$

The resulting far field is the sum of all individual contributions derived above.

III. RESULTS and CONCLUSIONS

Fig.2. shows the estimated radiation pattern in the azimuth plane for the following data at GSM frequency: w=34cm, h=7.5cm, d=8.5cm and f=880MHz. This result is compared with the MOM based solution of the commercial software package FEKO of EMSS (version 3.03). The agreement is good up to 60 degrees off the main peak. The mismatch between 60 and 70 degrees, where the observation point crossing the edges of the reflec-

tor, might be due to diffracted fields from the edges. It has been found that the diffracted field contribution is significant if the dimensions of the structure are comparable to wavelength. The estimation could be further improved by adding higher order reflecting fields.

REFERENCES

[1] C.A. Balanis and D. Decarlo, "Monopole antenna patterns on finite size composite ground planes", IEEE Trans. Antennas Propagat., Vol. 30, pp. 764 – 768, 1982.

[2] J.Huang, "The finite ground plane effect on the microstrip antenna radiation patterns", IEEE Trans. Antennas Propagat., Vol. 31, pp. 649 – 653, 1983.

[3] E. Lier and K.R. Jakobsen, "Rectangular microstrip patch antenna with infinite and finite ground plane dimensions", IEEE Trans. Antennas Propagat., Vol. 31, pp. 978 – 984, 1983.

[4] C.A. Balanis, " Radiation characteristics of current elements near a finite-length cylinder", IEEE Trans. Antennas Propagat., Vol. 18, pp. 352 – 359, 1970.

[5] W.D. Burnside, R.J. Marhefka, and L.Y. Chong, " Roll-Plane analysis of on-aircraft antennas", IEEE Trans. Antennas Propagat., Vol. 23, 309 – 316, 1975.

[6] T. Griesser and C.A. Balanis, "Reflections, diffractions, and surface waves for an interior impedance wedge of arbitrary angle", IEEE Trans. Antennas Propagat., Vol. 37, pp. 927-935, July 1989.

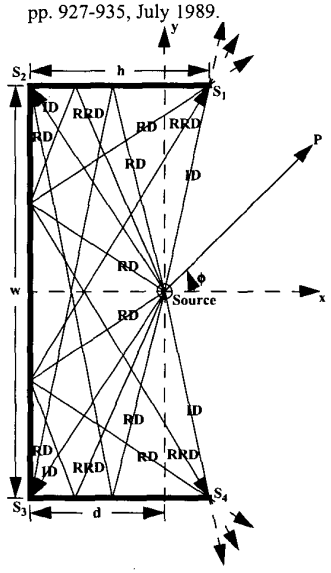

Fig. 1 Ray model of the dipole with Beam focusing structure.
ID – Incident Diffracted
RD – Refelected Diffracted
RRD – Reflected Reflected Diffracted

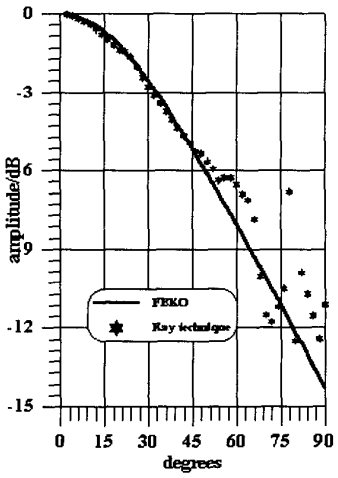

Fig. 2 Comparison of results obtained by this method (*) and FEKO (–).